Transient domain formation in membrane-bound organelles undergoing maturation

Serge Dmitrieff* and Pierre Sens†
Laboratoire Gulliver (CNRS UMR 7083) ESPCI, 10 rue Vauquelin, 75231 Paris Cedex 05, France
(Received 12 July 2012; revised manuscript received 25 August 2013; published 4 December 2013)

The membrane components of cellular organelles have been shown to segregate into domains as the result of biochemical maturation. We propose that the dynamical competition between maturation and lateral segregation of membrane components regulates domain formation. We study a two-component fluid membrane in which enzymatic reaction irreversibly converts one component into another and phase separation triggers the formation of transient membrane domains. The maximum domain size is shown to depend on the maturation rate as a power law similar to the one observed for domain growth with time in the absence of maturation, despite this time dependence not being verified in the case of irreversible maturation. This control of domain size by enzymatic activity could play a critical role in regulating exchange between organelles or within compartmentalized organelles such as the Golgi apparatus.

DOI: 10.1103/PhysRevE.88.062704 PACS number(s): 87.16.A−, 64.60.−i, 87.16.D−

I. INTRODUCTION

Molecules secreted and internalized by eukaryotic cells follow well-defined routes, the secretory or endocytic pathways, along which they are exposed to a succession of biochemical environments by sequentially visiting different membrane-bound organelles [1]. Different organelles have different membrane compositions, as well as a distinct set of membrane-associated proteins, referred to henceforth as the membrane *identity*. Interestingly, it has been shown that the identity of some organelles changes with time; for example, the early endosome (a compartment digesting newly internalized content) has a different identity from the late endosome, which then becomes a lysosome [2]. One fundamental issue underlying the organization of intracellular transport is whether progression along the various pathways occurs by exchange between organelles of fixed biochemical identities (via the budding and scission of carrier vesicles) or by the biochemical maturation of the organelles themselves [1,2]. This question is particularly debated for the Golgi apparatus, where proteins undergo post-transcriptional maturation and sorting. The Golgi is divided into early (*cis*), middle (*medial*) and late (*trans*) micrometer-size compartments called cisternae. In yeast, each cisterna appears to undergo independent biochemical maturation from a cis to a trans identity in less than 1 min [3,4]. In higher eukaryotes, the cisternae form a tight and polarized stack with cis and trans ends, through which proteins travel in about 20 min [5]. Whether transport through the stack occurs by intercisternal exchange or by the maturation of entire cisternae remains controversial [5].

Maturation in an organelle membrane causes different membrane identities to transiently coexist and may trigger the formation of transient membrane domains. Membrane components have indeed been seen to segregate into domains in both yeast [3,4] and mammalian Golgi cisternae [6]. This is the case of proteins of the Rab family, thought to be essential identity labels of cellular organelles [2]. The so-called *Rab cascade*, in which the activation of one Rab inactivates the preceding Rab along the pathway, is thought to permit the sequential maturation of the organelle identity [7]. Domains could also emerge from the maturation of ceramids (present in cis-Golgi) into sphingomyelin (present in trans-Golgi), as these two species are known to lead to domain formation on vesicles [8]. Finally, there is a continuous gradient of membrane thickness from cis- to trans-Golgi compartments [9] and thickness mismatch can lead to phase separation in model membranes [10].

It has been argued that membrane domains in organelles could undergo budding and scission and hence control interorganelle transport [11,12]. This raises the interesting possibility that the rate of domain formation could control the rate of transport. To quantitatively assess this possibility, we studied transient domain formation in an ideal two-component membrane. We consider an irreversible transformation (maturation) $A \rightarrow B$ taking place between two components, with A and B representing distinct biochemical identities, and we investigate the phase behavior of such a membrane.

The kinetics of phase separation in binary mixtures has been abundantly studied [13]. In the context of fluid membranes, hydrodynamic flows in the membrane and the surrounding media make the problem quite complex. Several dynamical regimes have been reported, and a unified picture has not yet emerged [14,15]. For deformable fluid membranes such as cellular membranes, the budding of membrane domains [16] makes the dynamics of phase separation even more complex [17–19]. Here, we study transient phase separation on flat membranes, and we implement membrane deformability at a phenomenological level by introducing a critical domain size beyond which flat domains are unstable. If domains reach such a size, they undergo a budding transition and may serve as transport intermediates, provided a scission mechanism (e.g., the activity of specialized proteins such as dynamin [20]) separates budded domains from the rest of the membrane.

The budding of membrane domains may, for instance, be driven by the line energy associated with domain boundaries [16], expressed as the domain line tension γ times the boundary length. Budding is resisted by the membrane bending rigidity κ and surface tension σ and will occur for a finite range

*serge.dmitrieff@embl.de
†pierre.sens@espci.fr

of domain size R [21]:

$$4\frac{\kappa}{\gamma} < R < 2\frac{\gamma}{\sigma}. \quad (1)$$

For typical values of the parameters, $\kappa \simeq 10 k_B T$ and $\gamma \simeq 1$ pN, the lower bound is a fraction of the typical organelle's size ($\sim\mu$m), and the scenario of a line tension induced domain pinching appears realistic. The upper bound could be restrictive in a system with low area/volume ratio, where pinching might increase membrane tension and lead to incomplete buds. This is often observed in artificial vesicles, but this constraint does not appear stringent in organelles such as the Golgi. We assume henceforth that the rate of membrane deformation is much faster than the rate of chemical maturation, so that only the lower bound of Eq. (1) is relevant.

In this article, we show that, in a membrane undergoing irreversible maturation, the maximal size of transient domains follows a power law with respect to the maturation rate. First, we illustrate two modes of domain growth in fluid membranes. We then show the influence of maturation on domain growth, and the predicted power laws are then confirmed numerically. Because budding depends on domain size, this means that organelle exchange can be controlled by the maturation rate.

II. PHASE SEPARATION KINETICS IN FLUID MEMBRANES

In order to elucidate the role of maturation, we only consider phase separation in a flat fluid membrane and we disregard the influence of the surrounding fluid. This approximation is valid for domains smaller than $\sim\eta_2/\eta_3$, where η_3 is the three-dimensional viscosity of the surrounding fluid (the cytoplasm and the lumen of cellular organelles in the cell) and η_2 is the two-dimensional viscosity of the membrane [22]. For lipid membranes, using $\eta_2 \simeq 10^{-9}$ Pa m s and $\eta_3 \simeq 10^{-3}$ Pa s [23], one expects $\eta_2/\eta_3 \simeq \mu m$.

Domain growth is initially dominated by the so-called "Ostwald ripening," where large domains grow by adsorbing diffusing matter evaporated from smaller domains. At later times, hydrodynamic effects, leading in particular to domain coalescence, dominate the growth. In both cases, after an early nucleation stage, the domain size R_c increases with time according to a power law [13]:

$$R_c^{1/\alpha-1}\dot{R}_c \propto \tilde{D}(\bar{\phi}) \Rightarrow R_c \sim t^{\alpha}. \quad (2)$$

The exponent α and the transport coefficient $\tilde{D}$ depend on the dominant growth process, and the latter also depends on composition, line tension, and component mobility.

A. Thermodynamics

The thermodynamics of phase separation in a two-component membrane containing distinct biochemical identities A and B can be studied using a local order parameter ϕ varying continuously between $\phi = 0$ for A-rich and $\phi = 1$ for B-rich membrane regions. We use the classical Landau free energy [13]:

$$\mathcal{F} = \int d^2\mathbf{r}\left[V[\phi(\mathbf{r})] + \frac{1}{2}\zeta\|\nabla\phi\|^2\right],$$
$$V[\phi] = \frac{k_B T}{a^2}\left[\phi\log\phi + (1-\phi)\log(1-\phi)\right] + \frac{K}{2a^2}\phi(1-\phi), \quad (3)$$

where $a \sim nm$ is a molecular size. This energy is the sum of an interfacial term (of parameter ζ) and a potential term V that includes the translational entropy and the interaction between the two phases (repulsive if $K > 0$).

Phase separation occurs spontaneously inside the spinodal region of the phase diagram, defined by $K > k_B T/[\bar{\phi}(1-\bar{\phi})]$, where $\bar{\phi}$ is the mean value of ϕ in the system [24]. Within this region, the interface between A-rich and B-rich domains (of densities ϕ_A and ϕ_B, respectively, see Fig. 1) is sharp and the energy of interaction reduces to a line energy characterized by the line tension γ, defined in Appendix A [Eq. (A3)].

B. Domain growth by Ostwald ripening

For a conserved order parameter, the dynamics of the order parameter is described by a Cahn-Hilliard equation [13]:

$$\partial_t\phi = D\nabla^2\mu/k_B T, \quad \mu = a^2\delta\mathcal{F}/\delta\phi, \quad (4)$$

where μ is the chemical potential associated with ϕ and D is the monomer diffusion coefficient. Within the two-phases region of Fig. 1, Eq. (4) produces domains with sharp boundaries. Domains larger than a critical size R_c grow at the expense of smaller domains, and interdomain exchange occurs by monomer diffusion through the bulk phase.

Provided diffusion is much faster than the evaporation of the smallest domains, Lifshitz, Slyozov, and Wagner (LSW) have shown that the characteristic domain size should obey the scaling law $R_c \sim t^{1/3}$ [25,26]. The detailed computation is presented Appendix A, but this result can be qualitatively explained: if diffusion is fast, the order parameter profile outside the domain boundary satisfies the quasistatic approximation $\nabla^2\mu = 0$, and the chemical potential inside the domain is related to the line tension by $\mu \approx \gamma/R_c$ [13]. If there is only one length scale R_c in the system, mass conservation implies

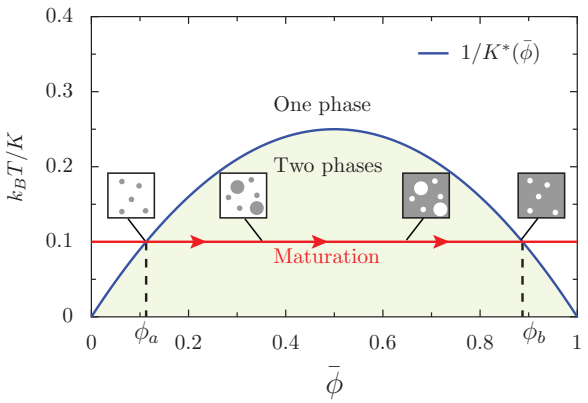

FIG. 1. (Color online) Phase diagram of a binary mixture undergoing chemical maturation. The blue line represents the spinodal line. The chemical reaction (maturation) increases the mean order parameter $\bar{\phi}$ from 0 to 1.

$\dot{R}_c \sim \nabla\mu \sim \mu/R_c$. Finally,

$$R_c^2 \dot{R}_c \propto D\gamma a^2/k_B T, \tag{5}$$

leading to the classical LSW dynamical scaling $R_c \sim t^{1/3}$ [25,26]. The size distribution of domains growing by Ostwald ripening is strongly peaked around the size R_c [13]. Though this was strictly shown in three dimensions or higher, it has been confirmed numerically in two dimensions [27].

A similar scaling has been observed numerically *at steady state* in the presence of reversible reaction $A \rightleftarrows B$, time being replaced by the inverse of the reaction rate [28]. In the following we show analytically and numerically that a similar scaling also exists for irreversible reactions.

C. Domain growth by coalescence

The role of hydrodynamics on phase separation in fluid membranes is still controversial, despite considerable recent attention [15,29]. For off-critical mixtures ($\phi \neq 1/2$), hydrodynamic correlations result in the diffusion and coalescence of entire domains. At the scaling level [13], the area of the largest domain can at most double at each coalescence event: $\dot{R}_c \leqslant R_c/\tau_D$. The typical collision time $\tau_D = L^2/D_d$ depends on the domain diffusion coefficient D_d and the typical area per domain $L^2 \sim R_c^2/\bar{\phi}$. Finally, one finds

$$R_c \dot{R}_c \propto D_d \bar{\phi}. \tag{6}$$

If viscous dissipation is mostly due to membrane hydrodynamics, the domain diffusion coefficient D_d is only weakly dependent on domain size [22]. One thus expects $R_c \sim t^{1/2}$ for constant composition, which dominates Ostwald ripening at long times.

The size distribution of domains can be studied using the Smoluchowski coagulation equation [30]:

$$\partial_t C_n = J_n - kC_n N + \frac{k}{2}\sum_{m=1}^{n-1} C_m C_{n-m},$$
$$\text{with} \quad N = \sum_{m=1}^{\infty} C_m, \tag{7}$$

where C_n is the concentration of domains containing n monomers (if R is the domain size: $n \sim R^2$), k is a typical diffusion rate, and domain scission has been neglected. This model has been studied extensively for different forms of the diffusion rate [31]. Following the assumption that the diffusion coefficient of a domain is independent of its size [22], we choose a constant diffusion rate $k = D_d/a^2$. J_n is a source and sink term allowing for the creation or removal of domains [32].

In the absence of maturation ($\bar{\phi} = \text{const.}$, $J_n = 0$), the size distribution is well approximated by an exponential with a characteristic domain size $\bar{n} \sim \bar{\phi} kt$, giving the domain radius $\bar{R}(t) \sim \sqrt{D_d \bar{\phi} t}$, in agreement with Eq. (6).

The domain size distribution is modified by the presence of sources and sinks. It has been shown in [32] that choosing a source and sink term that conserves the average concentration $\bar{\phi}$ (i.e., $J_n = j_{\text{in}}\delta_{n,1} - k_{\text{off}} C_n$) produces the steady-state power-law distribution $C_n \sim n^{-3/2}$, up to a characteristic domain size beyond which the distribution is exponential. The characteristic size obeys a scaling reminiscent of Eq. (6): $R_c \propto \sqrt{D_d \bar{\phi}/k_{\text{off}}}$.

III. TRANSIENT PHASE SEPARATION UNDER IRREVERSIBLE MATURATION

Maturation corresponds to the increase of $\bar{\phi}$ with time from $\bar{\phi} = 0$ to $\bar{\phi} = 1$ due to a chemical reaction. If $K > 4k_B T$, the spinodal line (Fig. 1) is crossed twice, first at $\bar{\phi} = \phi_A$ when phase separation starts and then at $\bar{\phi} = \phi_B$ where the system tends to be homogenous once again. We ask whether domains larger than a critical budding size, for instance, given by Eq. (1), can form during the time the system is prone to phase separation (i.e., while $\phi_A < \bar{\phi} < \phi_B$).

A. Dynamical scaling

For Ostwald ripening, the quasistatic approximation above assumes that the order parameter profile outside domains adjusts quasistatically to domain growth ($\nabla^2\phi = 0$ in the bulk). In a maturing membrane, the average membrane composition evolves according to $\partial_t \bar{\phi} = k_r(1 - \bar{\phi})$, and the quasistatic composition profile satisfies

$$D\nabla^2\mu + k_r(1 - \phi) = 0\,, \tag{8}$$

which defines a characteristic length scale $\lambda_D = \sqrt{D/k_r}$. It is shown in Appendix B that the growth of small domains with $R \ll (\lambda_D^2 \gamma a^2/k_B T)^{1/3}$ satisfies the dynamical scaling given by Eq. (2) with the LSW exponent $\alpha = 1/3$ and with a transport coefficient $\tilde{D}(\bar{\phi})$ depending on time only through the value of the mean concentration $\bar{\phi}$.

In the regime dominated by coalescence, Eq. (6), which assumes a single characteristic domain size, may be used with a time-dependent $\bar{\phi}$ under the assumption that the number of domains varies little between two coalescence events. This approximation is shown to be valid below.

The extent of phase separation can be characterized by the maximum size $R_{\max}$ a domain can reach during the transient phase separation. Here, we are interested in membrane domains that may undergo budding, namely, domains of the minority phase surrounded by the majority phase. Domains are thus of the mature species for $\phi < 1/2$ and of the immature species for $\phi > 1/2$ (see insets Fig. 1), and the maximum domain size occurs for $\phi = 1/2$. Integrating Eq. (2), one finds

$$R_{\max}^{1/\alpha} \propto \int_{\phi_A}^{1/2} \tilde{D}(\bar{\phi}) \frac{d\bar{\phi}}{\dot{\bar{\phi}}} = \frac{1}{k_r}\int_{\phi_A}^{1/2} \frac{\tilde{D}(\bar{\phi})}{1-\bar{\phi}} d\bar{\phi}. \tag{9}$$

The *maximum* size of transient domains in a maturing membrane is thus predicted to follow the dynamical scaling law observed for domain growth under fixed composition [Eq. (2)], where the maturation rate replaces $1/t$: $R_{\max} \sim k_r^{-\alpha}$. This dynamical scaling is reminiscent of the scaling observed *at steady state* in the presence of reversible reaction $A \rightleftarrows B$ [28] or continuous recycling [32]. That it is also applicable to irreversible reactions is remarkable, since the kinetics of domain growth in a membrane undergoing maturation do not follow the same scaling, as $\bar{\phi}$ changes with time. This kinetics is not easily obtained from scaling arguments for Ostwald ripening, as the $\bar{\phi}$ dependence of Eq. (5) is not straightforward (as shown in Appendix B). For domain coalescence, a simple

integration of Eq. (6) with $\bar{\phi} \simeq k_r t$, valid at early time, shows that one expects

$$R_c(t) \simeq t\sqrt{D_d k_r}. \tag{10}$$

This linear growth contrasts with the $\sim t^{1/2}$ scaling in the absence of maturation.

B. Numerical results: Ostwald ripening

The prediction of Eq. (9) was tested numerically. Without hydrodynamics, we performed Monte Carlo simulations of the Ising model with nearest-neighbor interaction (parameter J) and a discrete order parameter s (0 or 1):

$$\mathcal{H} = \frac{1}{2}\sum_{i,j} J[s_i(1-s_j) + s_j(1-s_i)]. \tag{11}$$

This is numerically simpler than the continuous Landau free energy Eq. (3) and was shown to be thermodynamically equivalent [33]. The line tension γ (in units of $k_B T/a$) can be related to J (normalized by $k_B T$) by $\gamma = 2J - \log[\coth(J)]$ [34].

Monomer diffusion is implemented using Kawasaki dynamics (spin exchange between nearest neighbors), known to produce the LSW growth in a system without maturation [27,35]. Maturation is implemented by letting each site with $s = 0$ become an $s = 1$ site with a probability $k_r dt$ at each time step (of duration dt). In order to be able to reach 10^7 time steps consistent with physiological recycling rates $[D/(k_r a^2) \sim 10^7]$ in a reasonable physical time, the simulation size is smaller than that of a real-life organelle (400×400, or about $1/6$ of a μm^2 cisterna for $a = 1$ nm). This is however not a serious drawback, as the domain size remains significantly smaller than the simulation size for all but the slowest maturation rate considered (see Fig. 3).

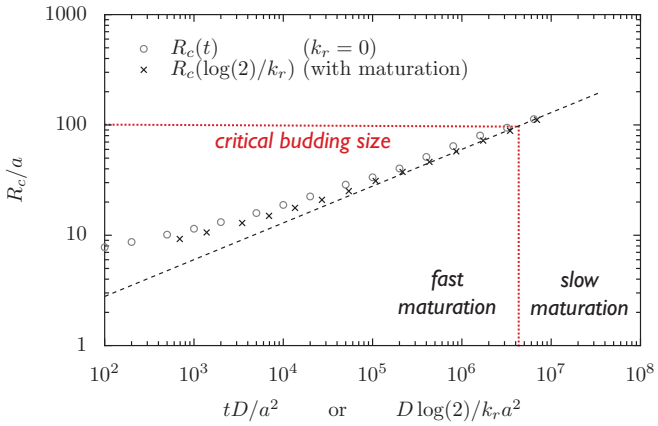

FIG. 3. (Color online) Growth by Ostwald ripening. Domain size (in units of the molecule size a) as a function of time (○) and maximum domain size as a function of the inverse maturation rate $1/k_r$ (×), from simulations with $J = 0.75$. Time is in units of the diffusion time a^2/D ($\approx 10^{-5}$ s). The dashed line corresponds to $k_r^{-1/3}$. The critical budding size is estimated based on the line-tension-driven budding scenario [Eq. (1)].

Snapshots of the simulations, shown in Fig. 2, highlight the similarity between a system without maturation (for $\bar{\phi} = 1/2$) after a time t and a system which reaches the same concentration by maturation (after a time $t = \log 2/k_r$). Figure 3 compares the variation of the average domain size with time in a system without maturation (with $\bar{\phi} = 1/2$) and the variation of the maximum domain size with respect to the inverse maturation rate in a system undergoing maturation. Both the LSW scaling without maturation ($R \sim t^{1/3}$) and our predicted scaling with maturation ($R_{\max} \sim k_r^{-1/3}$) are apparent at late stages. Strikingly, prefactors of the power law appear very similar with or without maturation.

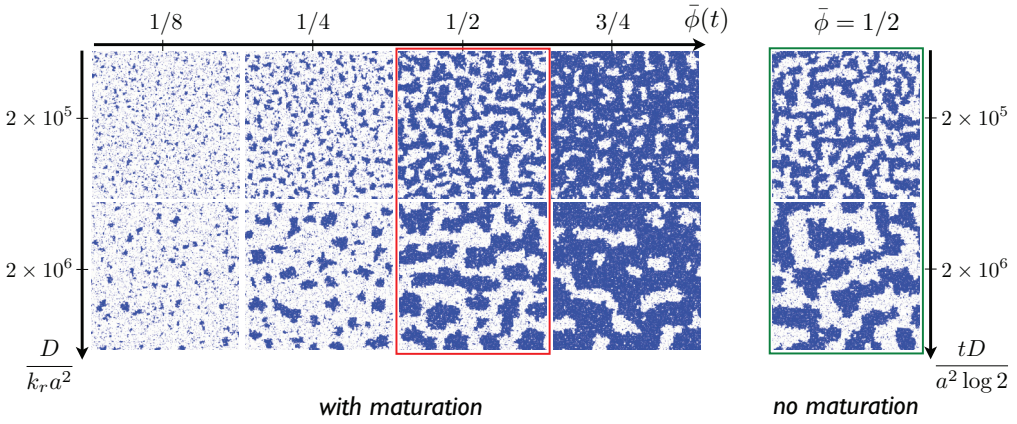

FIG. 2. (Color online) Growth by Ostwald ripening. Snapshots of Monte Carlo simulations of domain formation in a 400×400 Ising model with and without maturation. With maturation (left), snapshots of the system are shown for four different times (corresponding to the average compositions $\bar{\phi} = 1/8$, $1/4$, $1/2$, and $3/4$) and for two different maturation rates (top row, fast maturation; bottom row, slow maturation). The maximum domain size, obtained for $\bar{\phi} = 1/2$ (middle, red frame), is larger under slower maturation. Without maturation (right, green frame), two snapshots are shown for a fixed composition $\bar{\phi} = 1/2$ (top row, early time; bottom row, late time). The times are chosen such that they correspond to the times needed to reach $\bar{\phi} = 1/2$ under slow and fast maturation. This figure illustrates the correspondency between the domain growth with time under fixed composition $\bar{\phi} = 1/2$ in the absence of maturation (right, green frame), and the dependence of the maximum domain size with the maturation rate in the presence of maturation (middle, red frame). In all cases, the interaction parameter $J = 0.75 k_B T$ corresponds to a physiological line tension $\gamma \simeq 4$ pN.

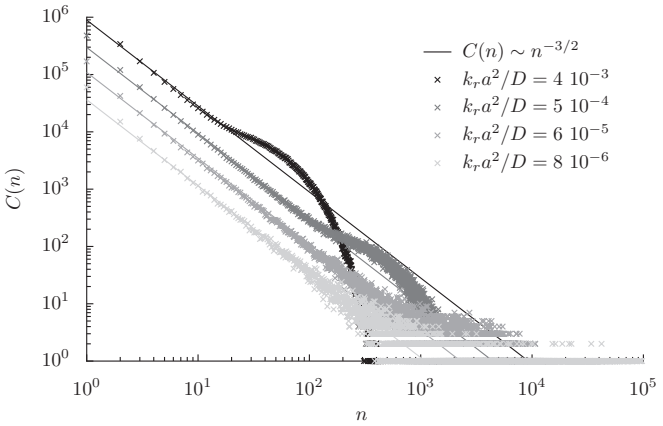

FIG. 4. Growth by coalescence. Distribution of domain size at $\bar{\phi} = 1/2$ for different maturation rates, obtained by numerically solving Eq. (7). The log-log plot shows a power-law behavior $\sim n^{-3/2}$ for small domains, as expected from scaling arguments.

C. Numerical results: Diffusion and coalescence

Growth by coalescence was studied numerically by solving a stochastic, discrete analog of the master equation, Eq. (7). We considered an assembly of N domains, a given domain encountering another given domain with a rate $k_1 = D_d/S = ka^2/S$, in which S is the effective system size (this assumes the domain diffusion coefficient to be size independent). The number of A molecules is $(1-\bar{\phi})S/a^2$ and each could be turned to B with a rate k_r (with $\bar{\phi} = \sum_n nC_n$). This was implemented using a Gillespie algorithm with $S/a^2 = 10^6$.

The system contains no mature components at $t = 0$ (i.e., $N = 0$). We find that the domain size distribution crosses over from a power-law $C_n = An^{-3/2}$ for small $n < n^*(t)$ to an exponential decay over the size n^* for large n. This result indicates that, in a system undergoing irreversible maturation, the domain size distribution is essentially stationary up to the crossover size $n^*(t)$, computed analytically below.

We first focus on the role of the maturation rate by analyzing domain size distribution for different values of k_r, after a time $t = \log 2/k_r$ for which $\bar{\phi}$ reaches $1/2$. This is when phase separation is most pronounced and one expects to observe the largest domains. Figure 4 shows the domain size distribution for $\bar{\phi} = 1/2$ for different values of the maturation rate. The power law $C_n = An^{-3/2}$ is confirmed up to a characteristic size that depends on k_r. This size may be computed as follows. Using Eq. (7) for $n = 1$, stationarity of the monomer concentration C_1 imposes $A \simeq k_r(1-\bar{\phi})/(kN)$, with the total number of domains $N = \sum_{n=1}^{\infty} C_n \simeq \sum_{n=1}^{n^*} C_n = \sqrt{(1-\bar{\phi})k_r/k}$. Using the conservation relation $\bar{\phi} = \sum_{n=1}^{\infty} nC_n \simeq \sum_{n=1}^{n^*} nC_n \simeq \sqrt{(1-\bar{\phi})k_r/kn^*}$, the maximum domain size is found to be $n^* \sim k/k_r \times \bar{\phi}^2/(1-\bar{\phi})$, and the average domain size is $\bar{n} \equiv \bar{\phi}/N = \sqrt{n^*}$. The maximum and average domain size when $\bar{\phi} = 1/2$ are predicted to depend on the maturation rate according to

$$R_{\max} \sim \sqrt{\frac{D_d}{k_r}} \quad \text{and} \quad \bar{R} \sim \left(\frac{D_d a^2}{k_r}\right)^{1/4}. \qquad (12)$$

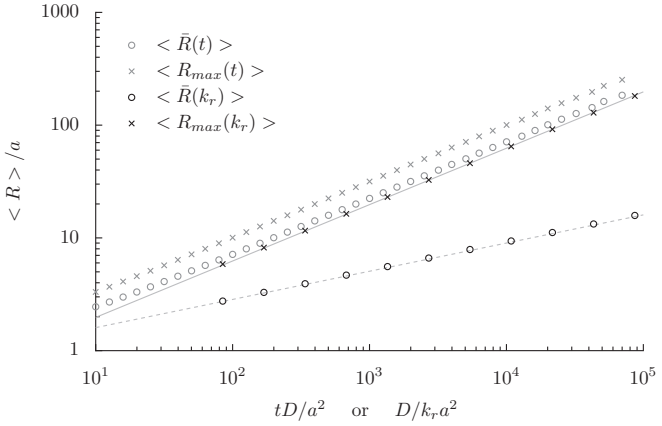

FIG. 5. Growth by coalescence. Mean domain size [$\bar{R}(t)$, gray circles] and maximum domain size [$R_{\max}(t)$, gray crosses] as a function of time in a system without maturation (constant $\bar{\phi}$), and mean domain size [$\bar{R}(k_r)$, black circles] and maximum domain size [$R_{\max}(k_r)$, black crosses] as a function of the inverse maturation rate $1/k_r$ in the presence of maturation. The dashed line is $\sim t^{1/4}$ and the solid line is $\sim t^{1/2}$.

These predictions are confirmed numerically in Fig. 5, which shows the variation of these two characteristic length scales with the maturation rate.

As discussed above, the dynamical scaling for domain growth can be obtained for the entire maturation process (at least while the matured species is the minority, $\bar{\phi} \in [0,1/2]$) using Eq. (6): $R_c \propto \sqrt{D_d k_r}\, t$. The characteristic domain size is predicted to increase linearly with time due to the combined effect of domain coalescence and the increasing fraction of matured species, both accounting for $\sqrt{t}$. This prediction was verified numerically, as shown in Fig. 6.

IV. DISCUSSION

The dynamical scaling predicted by Eq. (9) is thus universally observed whether domain growth proceeds by Ostwald ripening or by domain coalescence. On time scales consistent with biochemical maturation, $1/k_r \sim$ min, the maximum size

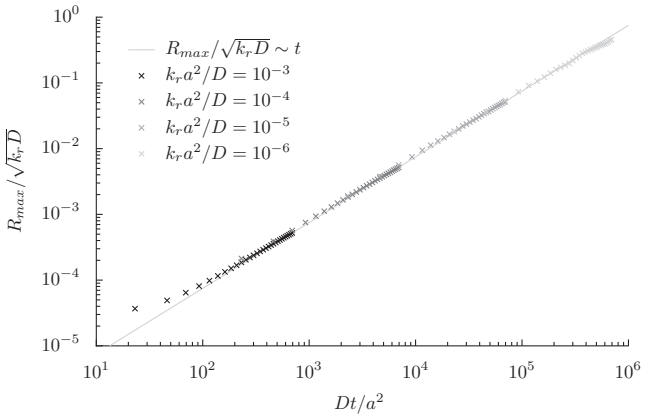

FIG. 6. Growth by coalescence. Variation of the maximum domain size as a function of time when maturation is present. The linear growth law $R_{\max}/\sqrt{k_r D} \sim t$ predicted in the text is observed. The maximum domain size is defined as $R_{\max} = \sqrt{\sum n^2 C_n/\bar{\phi}}$.

of transient domains in a membrane undergoing irreversible maturation is $\sim 0.1\ \mu$m with Ostwald ripening [Eq. (5) and Fig. 3] and $\sim 1\ \mu$m by domain coalescence [Eq. (6)], with $D = 0.1\ \mu\text{m}^2/\text{s}$, $a = 1$ nm, and $\gamma a/k_\text{B}T \sim 1$.

On deformable membranes, domains within the size range of Eq. (1) undergo line-tension-driven budding. Membrane deformability does not modify the early stages of domain growth, but has a complex influence on late-stage growth. Numerical studies report the possible fusion of budded domains [17–19], but membrane-mediated repulsion between nonflat domains may prevent their coalescence [36,37]. In low membrane tension organelles, domains large enough to deform will form a complete bud [21] that may undergo scission, and the late-stage dynamics should be less relevant.

Within our framework, one may expect irreversible maturation of membrane components to lead to domain budding and irreversible morphological changes if transient domains can reach the critical budding size, a possibility that requires slow maturation rates. This prediction could be tested experimentally on artificial membrane systems (giant unilamellar vesicles). We predict that a large ($\gtrsim \mu$m) deformable vesicle undergoing chemical maturation would preserve its integrity if the reaction were fast, while it would split in two or more daughter vesicles if the reaction were slower ($\gtrsim$min) and the maximum transient domain size exceeded the budding size. One possibility would be to use the sphingomyelinase-induced maturation of ceramid into sphingomyelin in giant vesicles, as this reaction is of physiological interest since it occurs in the Golgi apparatus and is known to produce lipid domains [38].

Extending our results to multicomponent cellular membranes is not straightforward, since many factors may influence domain growth and budding and participate in domain size regulation. Specific membrane proteins promote curvature and fission [39] and may modify the critical budding size range compared to Eq. (1). Interaction with the cytoskeleton may prevent domain diffusion and coalescence [40,41]. However, transient submicrometer domains have been seen on yeast Golgi cisternae [3,4] and slightly larger domains have been seen in mammals [6]. This suggests that domain formation is an important component impacting the dynamics of membrane-bound organelles. We thus venture the proposal that the rate of maturation of membrane components could fundamentally affect the morphology and dynamics of cellular organelles.

Our study appears particularly interesting in the case of the Golgi apparatus. We argue that the two extreme Golgi organizations observed in nature can be fitted within a single framework. Yeast Golgi (fast maturation, $k_r \sim 1/\text{min}$) could be made of dispersed cisternae undergoing independent maturation, because the maturation rate is too fast for the emergence of membrane domains that can reach the budding size. On the other hand, the fact that the Golgi of mammalian cells is a stack of interacting cisternae of different biochemical identities (cis, medial, trans) could be made possible by a relatively slow maturation rate ($k_r \sim 1/20$ min) allowing the formation of large mature domains. Although this simple picture is far from capturing the full complexity of the Golgi apparatus, and in particular the compositional complexity present in other models [42,43] or the recycling of resident Golgi enzymes by specific retrograde transport, our results suggest that an internal property of an organelle (the rate of chemical reaction in the Golgi apparatus) could control the structure and organization of this organelle.

ACKNOWLEDGMENTS

We gratefully acknowledge B. Goud, N. Gov, F. Perez, R. Phillips, and M. Rao for stimulating discussion.

APPENDIX A: LSW THEORY IN THE ABSENCE OF CHEMICAL REACTION

Following the method from Bray [13] (and the references therein), we compute the order parameter profile around a domain. Inside the spinodal region of the phase diagram (Fig. 1), obtained from the Landau free energy $\mathcal{F}$ given in Eq. (3), the potential energy $V(\phi)$ presents two local minima, for high and low values of ϕ (ϕ_1 and ϕ_0, respectively). In the following, lengths are normalized by the molecular size a and time by the characteristic diffusion time (a^2/D).

In the absence of maturation, the Cahn-Hilliard equation reads

$$\partial_t \phi = -\nabla \cdot \boldsymbol{j}, \quad \text{with} \quad \boldsymbol{j} = -\frac{D}{k_\text{B}T}\nabla\mu, \quad \text{and} \quad \mu = a^2\frac{\delta\mathcal{F}}{\delta\phi} = a^2[V'(\phi) - \zeta\nabla^2\phi], \tag{A1}$$

where $V'(\phi)$ is the derivative of the potential $V(\phi)$ with respect to ϕ.

We are interested in the growth of a ϕ-rich domain (say) with concentration close to ϕ_1, in a ϕ-poor bulk (of concentration ϕ_b close to ϕ_0). The radially symmetric stationary solution of Eq. (A1), $\nabla^2\mu = 0$, reads $\mu \sim 1/r^{d-2} + \text{const.}$, where $r = 0$ at the center of the domain and where d is the system's dimension. For the situation of interest to us ($d = 2$), the treatment below is not strictly valid, since the stationary solution shows logarithmic divergence, but it has been shown numerically to be marginally valid [13]. Well inside the spinodal region, one expects domains to be characterized by a sharp boundary between the rich and poor phases, located at $r = R$ (the domain size). Provided diffusion is fast compared to the kinetics of domain growth, the stationary solution is valid everywhere except at the domain boundary, where the concentration gradient is sharply peaked. Calling z the local coordinate normal to the boundary, one can write $\nabla^2\phi \simeq K\partial_z\phi + \partial_z^2\phi$, where $K = (d-1)/R$ is the interface curvature. The value of μ at the interface can be obtained by integrating $\partial_z\phi \times \mu$ [where μ is given by Eq. (A1)] across the interface noting that, unlike $\partial_z\phi$, μ and K vary smoothly across the interface. This yields the Gibbs-Thomson boundary condition [13]:

$$\mu_1 \Delta\phi = a^2(\Delta V - K\gamma), \tag{A2}$$

where μ_1 is the chemical potential inside the domain, Δ represents the difference between the domain and the bulk values, and γ is the line tension, defined as [13]

$$\gamma = \zeta\int_{-\infty}^{\infty} dz(\partial_z\phi)^2 = \int_{\phi_b}^{\phi_1} d\phi\sqrt{2\zeta V(\phi)}. \tag{A3}$$

Therefore, we may find the profile of μ, for a domain of size R, that satisfies the boundary conditions $\mu(r=0) = \mu_1$ and

$\mu(r \to \infty) =$ constant:

$$\mu(r < R) = \mu_1$$

$$\mu_1 = \frac{a^2}{\phi_b - \phi_1}[V(\phi_b) - V(\phi_1) - K\gamma] \quad \text{(A4)}$$

$$\mu(r > R) = a^2 V'(\phi_b) + [\mu_1 - a^2 V'(\phi_b)]\left(\frac{R}{r}\right)^{d-2}. \quad \text{(A5)}$$

The kinetics of domain growth ($\partial_t R \equiv v$) can be obtained by comparing the fluxes in and out of the interface. The interface velocity is proportional to the discontinuity of the potential gradient at the interface: $(\phi_1 - \phi_b)v = D/k_B T[\partial_r \mu]_{R-\epsilon}^{R+\epsilon}$ (with $\epsilon \to 0$). For $d > 2$, this yields

$$\dot{R} = \frac{D\gamma a^2 (d-1)(d-2)}{k_B T R(\phi_1 - \phi_b)^2}\left(\frac{1}{R_c} - \frac{1}{R}\right), \quad \text{(A6)}$$

$$\text{with} \quad R_c = \frac{(d-1)\gamma}{V(\phi_b) - V(\phi_1) - (\phi_b - \phi_1)V'(\phi_b)}.$$

Equation (A6) shows that domains smaller than the critical domain size R_c evaporate in the bulk, whereas larger domains grow. For small domains, $R^2\dot{R} \sim -t$ and hence their evaporation shows the scaling $R \sim -t^{1/3}$.

At equilibrium ($\phi_b = \phi_0$), the equality of chemical potentials between the ϕ-rich and ϕ-poor phases leads to $V(\phi_0) - V(\phi_1) - (\phi_0 - \phi_1)V'(\phi_0) = 0$ and $R_c \to \infty$. Finite size domains can grow if the bulk phase is supersaturated in the minority species: $\phi_b = \phi_0 + \epsilon$, with $\epsilon \ll \phi_1 - \phi_0$, in which case the critical radius is

$$R_c = \frac{(d-1)\gamma}{(\phi_1 - \phi_0)V''(\phi_0)\epsilon}. \quad \text{(A7)}$$

Supersaturation depends on the evaporation of small drops, hence on time. To obtain the growth law for the critical size $R_c(t)$, one has to consider an assembly of domains, characterized by a size distribution $n(R,t)$. If the scaling law

$$n(R,t) = \frac{1}{R_c(t)^{d+1}} f\left(\frac{R}{R_c(t)}\right) \quad \text{(A8)}$$

is assumed for the size distribution, the only growth law maintaining the scaling is $R_c \sim t^{1/3}$ [13]. Indeed, the continuity equation for $n(R,t)$ reads

$$\partial_t n + \partial_R [v(R)n(R)] = 0, \quad \text{(A9)}$$

where $v(R) = \dot{R}$. Injecting Eqs. (A6) and (A8) in Eq. (A9) yields a differential equation for f, which is time independent [consistent with the scaling hypothesis Eq. (A8)] only when

$$R_c^2 \dot{R}_c = A\frac{D\gamma a^2}{k_B T}, \quad \text{(A10)}$$

$$A = \alpha\frac{(d-1)(d-2)}{(\phi_1 - \phi_0)^2}, \quad \text{(A11)}$$

in which α is a numerical constant. This yields the Lifschitz-Slyozov-Wagner (L-S-W) scaling:

$$R_c \propto (\gamma t)^{1/3}. \quad \text{(A12)}$$

Because we assumed the scaling $n(R,t) = f[R/R_c(t)]$, the size of domains is distributed around R_c, and R_c is a good measure of the mean domain size. Although the previous treatment is strictly valid for $d > 2$ only, it has been shown that the scaling law should also be observed (within logarithmic corrections) for $d = 2$, as is the case for lipid membranes [13].

APPENDIX B: DOMAIN GROWTH WITH CHEMICAL MATURATION

In the presence of slow maturation, the chemical potential profile outside the domain is slightly modified as compared to Eq. (A5). The quasistationary solution of Eq. (8) reads

$$\mu(r > R) = A + B\left(\frac{R}{r}\right)^{d-2} - \frac{k_r}{2dD}r^2, \quad \text{(B1)}$$

where the constants A and B are given by boundary conditions. As in the absence of maturation, $\mu(R) = \mu_1$ at the domain's boundary. The chemical potential given by Eq. (B1) does not reach a constant value far from the domain's interface. We thus introduce the typical distance between two domains $2L$, and we require that $\mu(L) = \mu_b$, where L is given by $\bar{\phi}L^d = \phi_1 R^d + \phi_b(L^d - R^d)$.

Using these boundary conditions in Eq. (B1), we find

$$B = -\frac{1}{1 - (R/L)^{2-d}}\left\{\mu_b - \mu_1 + \frac{k_m}{2dD}L^2[1 - (R/L)^2]\right\}. \quad \text{(B2)}$$

At the lowest order in R/L, the extension of Eq. (A6) in the presence of maturation reads

$$\dot{R} = D(d-2)\frac{\mu_b - \mu_1}{R} + \frac{(d-2)k_r}{d}R\left(\frac{\phi_1}{\bar{\phi}}\right)^{2/d}, \quad \text{(B3)}$$

where μ_1 is given by Eq. (A4).

The first term of the right-hand side of Eq. (B3) corresponds to Ostwald ripening in the absence of maturation [Eq. (A6)] and produces a peaked domain size distribution with a characteristic size R_c given by Eq. (A12). The second term is due to maturation. It can be considered as a small correction provided $k_r R_c \ll \dot{R}_c \simeq D\gamma a^2/(k_B T R_c^2)$. We thus find that the LSW scaling [Eq. (A10)] should be valid in the presence of maturation provided

$$R_c \ll \left(\frac{D}{k_r}\frac{\gamma a}{k_B T}a\right)^{1/3} \simeq 10^2 a. \quad \text{(B4)}$$

[1] R. Kelly, Science **230**, 25 (1985).

[2] M. Zerial and H. McBride, Nat. Rev. Mol. Cell Biol. **2**, 107 (2001).

[3] K. Matsuura-Tokita, M. Takeuchi, A. Ichihara, K. Mikuriya, and A. Nakano, Nature (London) **441**, 1007 (2006).

[4] E. Losev, C. A. Reinke, J. Jellen, D. E. Strongin, B. J. Bevis, and B. S. Glick, Nature (London) **441**, 1002 (2006).

[5] S. Emr and other, J. Cell Biol. **187**, 449 (2009).

[6] G. Patterson, K. Hirschberg, R. Polishchuk, D. Gerlich, R. Phair, and J. Lippincott-Schwartz, Cell **133**, 1055 (2008).

[7] F. Rivera-Molina and P. Novick, Proc. Natl. Acad. Sci. U.S.A. **106**, 14408 (2009).
[8] J. Sot, L. Bagatolli, F. Goñi, and A. Alonso, Biophys. J. **90**, 903 (2006).
[9] K. Mitra, I. Ubarretxena-Belandia, T. Taguchi, G. Warren, and D. M. Engelman, Proc. Natl. Acad. Sci. U.S.A. **101**, 4083 (2004).
[10] F. Heberle, R. Petruzielo, J. Pan, P. Drazba, N. Kučerka, R. Standaert, G. Feigenson, and J. Katsaras, J. Am. Chem. Soc. **135**, 6853 (2013).
[11] K. Simons and M. J. Gerl, Nat. Rev. Mol. Cell Biol. **11**, 688 (2010).
[12] S. Pfeffer, Proc. Natl. Acad. Sci. U.S.A. **107**, 19614 (2010).
[13] A. Bray, Adv. Phys. **43**, 357 (1994).
[14] B. A. Camley and F. L. H. Brown, Phys. Rev. Lett. **105**, 148102 (2010).
[15] J. Fan, T. Han, and M. Haataja, J. Chem. Phys. **133**, 235101 (2010).
[16] R. Lipowsky, J. Phys. II (France) **2**, 1825 (1992).
[17] P. B. Sunil Kumar and M. Rao, Phys. Rev. Lett. **80**, 2489 (1998).
[18] P. B. Sunil Kumar, G. Gompper, and R. Lipowsky, Phys. Rev. Lett. **86**, 3911 (2001).
[19] M. Laradji and P. B. Sunil Kumar, Phys. Rev. Lett. **93**, 198105 (2004).
[20] S. M. Ferguson and P. D. Camilli, Nat. Rev. Mol. Cell Biol. **13**, 75 (2012).
[21] P. Sens and M. S. Turner, Phys. Rev. E **73**, 031918 (2006).
[22] P. Saffman and M. Delbrück, Proc. Natl. Acad. Sci. U.S.A. **72**, 3111 (1975).
[23] P. Cicuta, S. Keller, and S. Veatch, J. Phys. Chem. B **111**, 3328 (2007).
[24] P. Chaikin and T. Lubensky, *Principles of Condensed Matter Physics* (Cambridge University Press, Cambridge, UK, 1995).
[25] I. Lifshitz and V. Slyozov, J. Phys. Chem. Solids **19**, 35 (1961).
[26] C. Wagner, Z. Elektrochem. **65**, 581 (1961).
[27] D. A. Huse, Phys. Rev. B **34**, 7845 (1986).
[28] S. C. Glotzer, E. A. Di Marzio, and M. Muthukumar, Phys. Rev. Lett. **74**, 2034 (1995).
[29] B. Camley and F. Brown, J. Chem. Phys. **135**, 225106 (2011).
[30] M. v. Smoluchowski, Z. Phys. **17**, 557 (1916).
[31] S. C. Davies, J. King, and J. Wattis, J. Eng. Math. **36**, 57 (1999).
[32] M. S. Turner, P. Sens, and N. D. Socci, Phys. Rev. Lett. **95**, 168301 (2005).
[33] S. Safran, *Statistical Thermodynamics of Surfaces, Interfaces, and Membranes* (Westview Press, Boulder, CO, 2003).
[34] L. Onsager, Phys. Rev. **65**, 117 (1944).
[35] F. Krząkała, Phys. Rev. Lett. **94**, 077204 (2005).
[36] M. Yanagisawa, M. Imai, T. Masui, S. Komura, and T. Ohta, Biophy. J. **92**, 115 (2007).
[37] T. Ursell, W. Klug, and R. Phillips, Proc. Natl. Acad. Sci. U.S.A. **106**, 13301 (2009).
[38] M.-L. Fanani, L. D. Tullio, S. Hartel, J. Jara, and B. Maggio, Biophys. J. **67**, 67 (2009).
[39] H. T. McMahon and J. L. Gallop, Nature (London) **438**, 590 (2005).
[40] T. Fischer and R. L. C. Vink, J. Chem. Phys. **134**, 055106 (2011).
[41] J. Ehrig, E. Petrov, and P. Schwille, Biophys. J. **100**, 80 (2011).
[42] R. Heinrich and T. A. Rapoport, J. Cell Biol. **168**, 271 (2005).
[43] H. Gong, D. Sengupta, A.Linstedt, and R. Schwartz, Biophys. J. **95**, 1674 (2008).